THE JOURNAL OF BIOLOGICAL CHEMISTRY VOL. 288, NO. 6, pp. 4066–4075, February 8, 2013

Ligand-dependent Conformational Changes in the Clamp Region of the Cardiac Ryanodine Receptor*

Received for publication, October 13, 2012, and in revised form, December 17, 2012 Published, JBC Papers in Press, December 20, 2012, DOI 10.1074/jbc.M112.427864

Xixi Tian[‡1], **Yingjie Liu**[‡], **Ying Liu**[§], **Ruiwu Wang**[‡], **Terence Wagenknecht**[§¶], **Zheng Liu**[§2], **and S. R. Wayne Chen**[‡3]

From the [‡]*Libin Cardiovascular Institute of Alberta, Department of Physiology and Pharmacology and Department of Biochemistry and Molecular Biology, University of Calgary, Calgary, Alberta T2N 4N1, Canada,* [§]*Wadsworth Center, New York State Department of Health, Albany, New York 12201, and the* [¶]*Department of Biomedical Sciences, School of Public Health, State University of New York, Albany, New York 12201*

Background: Global structural changes occur in the ryanodine receptor (RyR) upon ligand activation.
Results: Different ligands induce different conformational changes in the clamp region of RyR.
Conclusion: Conformational changes in the clamp region of RyR are ligand-dependent.
Significance: RyR possesses multiple, ligand-dependent gating mechanisms associated with distinct structural changes.

Global conformational changes in the three-dimensional structure of the Ca^{2+} release channel/ryanodine receptor (RyR) occur upon ligand activation. A number of ligands are able to activate the RyR channel, but whether these structurally diverse ligands induce the same or different conformational changes in the channel is largely unknown. Here we constructed a fluorescence resonance energy transfer (FRET)-based probe by inserting a CFP after residue Ser-2367 and a YFP after residue Tyr-2801 in the cardiac RyR (RyR2) to yield a CFP- and YFP-dual labeled RyR2 ($RyR2_{Ser\text{-}2367\text{-}CFP/Tyr\text{-}2801\text{-}YFP}$). Both of these insertion sites have previously been mapped to the "clamp" region in the four corners of the square-shaped cytoplasmic assembly of the three-dimensional structure of RyR2. Using this novel FRET probe, we monitored the extent of conformational changes in the clamp region of $RyR2_{Ser\text{-}2367\text{-}CFP/Tyr\text{-}2801\text{-}YFP}$ induced by various ligands. We also monitored the extent of Ca^{2+} release induced by the same ligands in HEK293 cells expressing $RyR2_{Ser\text{-}2367\text{-}CFP/Tyr\text{-}2801\text{-}YFP}$. We detected conformational changes in the clamp region for the ligands caffeine, aminophylline, theophylline, ATP, and ryanodine but not for Ca^{2+} or 4-chloro-*m*-cresol, although they all induced Ca^{2+} release. Interestingly, caffeine is able to induce further conformational changes in the clamp region of the ryanodine-modified channel, suggesting that ryanodine does not lock RyR in a fixed conformation. Our data demonstrate that conformational changes in the clamp region of RyR are ligand-dependent and suggest the existence of multiple ligand dependent RyR activation mechanisms associated with distinct conformational changes.

The ryanodine receptor (RyR)[4] Ca^{2+} release channel plays an important role in excitation-contraction coupling in muscles and Ca^{2+} signaling in neurons and various non-excitable cells (1, 2). RyR is located in the sarcoplasmic or endoplasmic reticulum (ER) and mediates the release of Ca^{2+} from these intracellular stores (1, 3). The activity of RyR is tightly controlled by various physiological ligands to ensure proper sarcoplasmic reticulum/ER Ca^{2+} release (3, 4). RyR can also be modulated by a number of pharmacological ligands (5, 6). Altered RyR regulation by physiological ligands or abnormal RyR response to pharmacological ligands has been linked to muscle disorders such as heart failure, cardiac arrhythmias, and malignant hyperthermia (5, 7–11). Despite its important physiological and pathophysiological significance, the molecular mechanism of ligand modulation of RyR is largely undefined.

Functional and biochemical studies have demonstrated that many physiological and pharmacological ligands induce Ca^{2+} release by directly interacting with RyRs (3, 5, 6). A fundamental unresolved question is how this large array of ligands with diverse structures activates the RyR channel. It is thought that RyR contains ligand-specific binding sites and that ligand binding to these sites induces conformational changes in the channel that consequently lead to the opening of the channel gate and Ca^{2+} release (12–17). Considerable efforts over the past decades have been focused on the understanding of ligand-induced conformational changes in RyR. Ikemoto and co-workers (12, 13, 16) labeled RyR with a thiol-reacting fluorescent probe and showed that channel ligands such as Ca^{2+} and ATP changed the fluorescence intensity of the labeled RyR, suggesting ligand-induced conformational changes in RyR. Consistent with these biochemical studies, cryo-electron microscopy (cryo-EM) and single particle image analysis also revealed major structural rearrangements in the three-dimensional structure of RyR upon binding of ryanodine and Ca^{2+} or binding of a non-hydrolyzable analog of ATP, AMP-PCP, and Ca^{2+}

* This work was supported, in whole or in part, by National Institutes of Health Grants R01HL095541 (to Z. L.) and R01AR040615 (to T. W.). This work was also supported by research grants from the Canadian Institutes of Health Research and the Heart and Stroke Foundation of Alberta NWT and Nunavut (to S. R. W. C.).

[1] Recipient of an Alberta Innovates-Health Solutions Studentship Award.
[2] To whom correspondence may be addressed. Tel.: 518-486-2712; Fax: 518-473-2900; E-mail: liuz@wadsworth.org.
[3] An Alberta Innovates-Health Solutions Scientist. To whom correspondence may be addressed: HRIC GAC58, 3330 Hospital Dr. NW, Calgary, AB, Canada. Tel.: 403-220-4235; Fax: 403-270-0313; E-mail: swchen@ucalgary.ca.

[4] The abbreviations used are: RyR, ryanodine receptor; cryo-EM, cryo-electron microscopy; 4-CmC, 4-chloro-*m*-cresol; ICM, intracellular-like medium; SOICR, store-overload induced Ca^{2+} release; ER, endoplasmic reticulum; AMP-PCP, adenosine 5′-(β,γ-methylene)triphosphate; KRH, Krebs-Ringer Hepes; CFP, cyan fluorescent protein; YFP, yellow fluorescent protein.

to the channel (14, 15, 18, 19). Particularly, large conformational changes were observed in the transmembrane domain and in the four corners of the square-shaped cytoplasmic assembly, also known as clamp regions, in the three-dimensional architecture of RyR. Substantial structural rearrangements in the clamp region, the central cytoplasmic region, and the transmembrane domain were also detected when RyR was activated by another channel ligand, PCB 95 (17). Hence, these studies clearly demonstrate that conformational changes occur in RyR upon ligand binding.

An increasing body of evidence suggests that the clamp region consists of several key structural domains that are crucial for channel regulation and gating. It has recently been proposed that the clamp region contains the phosphorylation domain of RyR (20). Consistent with this prediction, residue Tyr-2801 in the cardiac RyR (RyR2), close to the Ser-2808 phosphorylation site, has been mapped to the clamp region (21). The central disease-causing mutation hotspot and one of the divergent regions (DR2) have also been localized to this region (22, 23). Based on the spacing of the dihydropyridine receptor (DHPR) arrangement in tetrads and that of the homotetrameric RyR, the clamp region has also been implicated in the activation of RyRs by DHPRs during excitation-contraction coupling in skeletal muscle (15, 24–26). The clamp region also harbors the binding sites for the chloride intracellular channel 2 (CLIC2) and the natrin toxin, a cysteine-rich secretory protein isolated from snake venom, both of which have been shown to modulate the activity of RyR (27, 28). Thus, studying conformational changes in the clamp region is likely to yield important insights into the mechanism of ligand-dependent gating of RyR.

Although cryo-EM studies revealed ligand-induced structural rearrangements in the clamp region, little is known about the ligand dependence of these conformational changes and their correlation with function. In this study we employed the fluorescent resonance energy transfer (FRET) approach to determining conformational changes in the clamp region of RyR2 upon binding with various ligands in live cells. The ligand-induced conformational changes were then correlated with the extent of Ca^{2+} release induced by the same ligand. To monitor conformational changes in the clamp region, we constructed a FRET probe in the clamp region by inserting a CFP after residue Ser-2367 and a YFP after residue Tyr-2801; both of these insertion sites have been previously mapped to the clamp region by cryo-EM (21, 23). Using this novel FRET probe, we found that caffeine, ATP, and ryanodine induced conformational changes in the clamp region and Ca^{2+} release in HEK293 cells, whereas Ca^{2+} and 4-chloro-*m*-cresol (4-CmC) induced Ca^{2+} release but caused no detectable conformational changes in the clamp region. Our results indicate that conformational changes in the clamp region are ligand-dependent and that RyR can be activated by different mechanisms associated with different conformational changes in the channel structure.

EXPERIMENTAL PROCEDURES

Construction of the CFP- and YFP-dual-labeled RyR2—The cloning and construction of the 15-kb full-length cDNA encoding the mouse cardiac RyR2 has been described previously (29). The RyR2 $_{\text{Ser-2367-CFP}}$ and $\text{RyR2}_{\text{Tyr-2801-YFP}}$ cDNAs were constructed according to the previously described procedures (21, 23). To generate the cDNA construct of $\text{RyR2}_{\text{Ser-2367-CFP/Tyr-2801-YFP}}$, the full-length RyR2 cDNA containing Ser-2367-CFP in pcDNA3 was released by the NheI-NotI restriction digestion and subcloned to the pBluescript vector. A cDNA fragment containing Tyr-2801-YFP was introduced into $\text{RyR2}_{\text{Ser-2367-CFP}}$ via the SphI restriction sites to form the full-length RyR2 containing both Ser-2367-CFP and Tyr-2801-YFP. The full-length $\text{RyR2}_{\text{Ser-2367-CFP/Tyr-2801-YFP}}$ construct was then transferred from pBluescript to pcDNA3 or pcDNA5 for transient transfection or generation of stable cell lines. The truncated RyR2, RyR2-(1–4770), was generated as described previously (30). The BsiWI (8864)-NotI (vector) DNA fragment from the RyR2-(1–4770) construct was used to replace the corresponding fragment in the full-length $\text{RyR2(wt)}_{\text{Ser-2367-CFP/Tyr-2801-YFP}}$ cDNA to yield the RyR2-(1–4770)$_{\text{Ser-2367-CFP/Tyr-2801-YFP}}$ construct. The sequences and the orientation of the inserted CFP or YFP cDNA were verified by DNA sequencing analysis.

Cell Culture, DNA Transfection, and Caffeine-induced Ca^{2+} Release Assay—HEK293 cells were maintained in Dulbecco's modified Eagle's medium as described previously (31). HEK293 cells grown on 100-mm tissue culture dishes for 18–20 h after subculture were transfected with 12 μg of RyR2(wt) or $\text{RyR2}_{\text{Ser-2367-CFP/Tyr-2801-YFP}}$ using calcium phosphate precipitation. Measurements of free cytosolic Ca^{2+} concentrations in the transfected HEK293 cells using the fluorescent Ca^{2+} indicator dye Fluo 3-AM were carried out as described previously (32). Briefly, the cells grown for 18–20 h after transfection were washed 4 times with phosphate-buffered saline (PBS) (137 mM NaCl, 8 mM Na_2HPO_4, 1.5 mM KH_2PO_4, and 2.7 mM KCl) and incubated in Krebs-Ringer Hepes buffer (KRH; 125 mM NaCl, 5 mM KCl, 1.2 mM KH_2PO_4, 6 mM glucose, 1.2 mM $MgCl_2$, 2 mM $CaCl_2$, and 25 mM Hepes, pH 7.4) without $MgCl_2$ and $CaCl_2$ at room temperature for 40 min and then at 37 °C for 40 min. After being detached from culture dishes by pipetting, cells were collected by centrifugation at 1000 rpm for 2 min in a Beckman TH-4 rotor. Cell pellets were washed twice with KRH buffer and loaded with 10 μM Fluo 3-AM in KRH buffer plus 0.1 mg/ml BSA and 250 μM sulfinpyrazone at room temperature for 60 min followed by washing with KRH buffer 3 times and resuspended in 150 μl of KRH buffer plus 0.1 mg/ml BSA and 250 μM sulfinpyrazone. The Fluo-3 loaded cells were added to 2 ml (final volume) of KRH buffer and challenged with various concentrations of caffeine in a cuvette. Fluorescence intensity of Fluo-3 at 530 nm was measured in an SLM-Aminco series 2 luminescence spectrometer with 480-nm excitation at 25 °C (SLM Instruments, Urbana, IL).

Generation of Stable, Inducible HEK293 Cell Lines—Stable, inducible HEK293 cell lines expressing RyR2(wt) or $\text{RyR2}_{\text{Ser-2367-CFP/Tyr-2801-YFP}}$ were generated using the Flp-In T-REx Core kit from Invitrogen. Briefly, Flp-In T-REx-293 cells were co-transfected with the inducible expression vector pcDNA5/FRT/TO containing the mutant cDNAs and the pOG44 vector encoding the Flp recombinase in 1:5 ratios using the calcium phosphate precipitation method. The transfected cells were washed with PBS 24 h after transfection followed by a change into fresh media for 24 h. The cells were then washed

again with PBS, harvested, and plated onto new dishes. After the cells had attached (~4 h), the growth medium was replaced with a selection medium containing 200 μg/ml hygromycin (Invitrogen). The selection medium was changed every 3–4 days until the desired number of cells was grown. The hygromycin-resistant cells were pooled, aliquoted, and stored at −80 °C. These positive cells are believed to be isogenic because the integration of RyR2 cDNA is mediated by the Flp recombinase at a single FRT site.

Single cell Luminal Ca^{2+} Imaging of HEK293 Cells—Luminal Ca^{2+} levels in HEK293 cells expressing RyR2(wt) or $RyR2_{Ser\text{-}2367\text{-}CFP/Tyr\text{-}2801\text{-}YFP}$ were measured using single cell Ca^{2+} imaging and the FRET-based ER luminal Ca^{2+}-sensitive cameleon protein D1ER as described previously (33). The cells were grown to 95% confluence in a 75 cm^2 flask, split with PBS, and plated in 100-mm tissue culture dishes at ~10% confluence 18~20 h before transfection with D1ER cDNA. After transfection for 24 h, the growth medium was then changed to an induction medium containing 1 μg/ml tetracycline (Sigma). After being induced for ~22 h, in intact cell studies, the cells were perfused continuously with KRH buffer containing 1 mM $CaCl_2$ and caffeine at various concentrations (1, 3, 5, and 10 mM), aminophylline (10 mM), or theophylline (10 mM) at room temperature (22 °C). In permeabilized cells studies, the cells were first permeabilized by 50 μg/ml saponin in an incomplete intracellular-like medium (incomplete ICM containing 125 mM KCl, 19 mM NaCl, and 10 mM HEPES, pH 7.4, with KOH) for 3–4 min. The cells were then switched to a complete ICM (incomplete ICM plus 2 mM ATP, 2 mM $MgCl_2$, and 0.05 mM EGTA, and 200 nM free Ca^{2+}, pH 7.4, with KOH) for 5–6 min to remove the saponin in the buffer. The permeabilized cells were then challenged with caffeine (10 mM), 4-CmC (1 mM), ATP (5 mM), Ca^{2+} (1 μM), or ryanodine (100 μM) plus caffeine (10 mM). Images were captured by a QuantEM 512SC camera every 2 s using the NIS-Elements AR software. The cells were excited at 430 nm, and the emission was split into 465- and 535-nm beams by a dual view device (Photometrics) placed in a Nikon eclipse Ti microscope equipped with the QuantEM 512SC camera. D1ER signals were determined from the ratios of the emissions at 535 ± 30 nm (YFP) and 465 ± 30 nm (CFP).

Measurements of FRET Signals from the Ser-2367-CFP/Tyr-2801-YFP FRET Pair—FRET signals from the Ser-2367-CFP/Tyr-2801-YFP FRET pair were measured using two approaches. In the first approach we determined the acceptor-donor emission ratio, *i.e.* the emission ratio of YFP and CFP fluorescence after CFP excitation only in intact or permeabilized HEK293 cells expressing $RyR2_{Ser\text{-}2367\text{-}CFP/Tyr\text{-}2801\text{-}YFP}$ as described above for measuring ER luminal Ca^{2+} using D1ER. To increase the expression level of $RyR2_{Ser\text{-}2367\text{-}CFP/Tyr\text{-}2801\text{-}YFP}$ and thus the fluorescence signals, HEK293 cells were induced by 1 μg/ml tetracycline for 2 days. In the second approach, HEK293 cells grown for 24–48 h after transfection with $RyR2_{Ser\text{-}2367\text{-}CFP/Tyr\text{-}2801\text{-}YFP}$ were washed 3 times with KRH buffer without $MgCl_2$ or $CaCl_2$ and examined on a Leica TCS SP5 confocal laser scanning microscope with a 63×/NA1.4 oil-immersion objective lens (34). Cells were kept at 37 °C using a water-heated stage incubator. To test the impact of RyR2 ligands on FRET, buffer in the cultured dishes was exchanged by peristaltic pumps. We utilized the acceptor photobleaching method to detect and measure FRET signals in the live cells. Briefly, CFP and YFP were excited with separate laser channels of 458 and 514 nm, respectively. Emission fluorescence intensity data were obtained at 465–495 nm (CFP) and 520–550 nm (YFP). We used a 700-Hz line frequency scan speed with bidirectional scan mode in combination with an image format of 1024 × 1024 pixels, which can record one image every 754 ms. Repeated scans (30–60) with maximum laser intensity at 514 nm were used to photobleach YFP, which lasted about 23–45 s, and the FRET efficiency was calculated according to the equation,

$$E = \left(\frac{I_{CFPpost} - I_{CFPpre}}{I_{CFPpost}}\right) \times 100\% \qquad \text{(Eq. 1)}$$

where I_{CFPpre} and $I_{CFPpost}$ are the respective background-corrected CFP fluorescence intensities before and after photobleaching YFP (35). The photobleaching, fluorescence intensity measurements and FRET efficiency calculation were controlled automatically by the software Leica Application Suite Advanced Fluorescence (LAS AF).

[^{3}H]Ryanodine Binding—HEK293 cells expressing $RyR2_{Ser\text{-}2367\text{-}CFP/Tyr\text{-}2801\text{-}YFP}$ for 2 days were collected in a 50-ml tube and permeabilized by 50 μg/ml saponin in an incomplete ICM buffer for 3 min. After saponin was washed off, the cells were apportioned equally into two 50-ml tubes. The two tubes of cells were incubated in a complete ICM buffer with or without 100 μM ryanodine plus 10 mM caffeine for 10 min. The ryanodine-treated or non-treated cells were washed with the complete ICM buffer to remove caffeine and free ryanodine. The washed cells were solubilized with the lysis buffer containing 25 mM Tris, 50 mM HEPES, pH 7.4, 137 mM NaCl, 1% CHAPS, 0.5% egg phosphatidylcholine, 2.5 mM DTT, and a protease inhibitor mix (1 mM benzamidine, 2 μg/ml leupeptin, 2 μg/ml pepstatin A, 2 μg/ml aprotinin, and 0.5 mM PMSF) on ice for 15 min. Cell lysate was obtained after removing the unsolubilized materials by centrifugation in a microcentrifuge at 4 °C for 2 min. Equilibrium [^{3}H]ryanodine binding to cell lysates was performed as described previously (32) with some modifications. [^{3}H]Ryanodine binding was carried out in a total volume of 600 μl of binding solution containing 60 μl of cell lysate, 500 mM KCl, 25 mM Tris, 50 mM Hepes, pH 7.4, 30 μM Ca^{2+}, 10 mM caffeine, 5 nM [^{3}H]ryanodine, and a protease inhibitor mix at 37 °C for 20 min. The binding mix was diluted with 5 ml of ice-cold washing buffer containing 25 mM Tris, pH 8.0, and 250 mM KCl and immediately filtered through Whatman GF/B filters presoaked with 1% polyethyleneimine. The filters were washed three times, and the radioactivities associated with the filters were determined by liquid scintillation counting. Nonspecific binding was determined by measuring [^{3}H]ryanodine binding in the presence of 50 μM unlabeled ryanodine. All binding assays were done in duplicate.

Statistical Analysis—All values shown are the mean ± S.E. unless indicated otherwise. To test for differences between groups, we used Student's *t* test (2-tailed) or one-way analysis of variance with a post hoc test. A p value <0.05 was considered to be statistically significant.

RESULTS

Construction of a FRET Probe in the Clamp Region of RyR2

The clamp region located at the corners of the square-shaped three-dimensional structure of RyR has been shown to display major structural rearrangements when the channel transitions from the closed to the open state (14, 15, 18, 19). The clamp region thus represents a potential location for building a FRET-based probe for sensing the conformational changes in RyR. We have previously mapped the three-dimensional locations of a number of GFPs inserted into different sites in the primary sequence of RyR2 (21–23, 36–39). Two of these GFPs, one inserted after residue Ser-2367 (Ser-2367-GFP) and the other after residue Tyr-2801 (Tyr-2801-GFP), were located close to each other (30 Å center to center) in the clamp region (21, 23). Thus, Ser-2367 and Tyr-2801 represent two suitable sites for inserting a pair of fluorescent proteins to build a FRET probe in the clamp region. To this end we inserted a CFP after residue Ser-2367 (Ser-2367-CFP) and a YFP after residue Tyr-2801 (Tyr-2801-YFP) to generate the dual CFP- and YFP-labeled RyR2, $RyR2_{Ser\text{-}2367\text{-}CFP/Tyr\text{-}2801\text{-}YFP}$ (Figs. 1, *A* and *B*). Fig. 1*C* shows that $RyR2_{Ser\text{-}2367\text{-}CFP/Tyr\text{-}2801\text{-}YFP}$ forms a functional Ca^{2+} release channel in HEK293 cells with a caffeine response similar to that of RyR2(wt). Note that the level of Ca^{2+} release induced by 2.5 or 5.0 mM caffeine is lower than that induced by the prior addition of 1.0 mM caffeine due to ER Ca^{2+} store depletion caused by the preceding cumulative additions of caffeine. To assess whether $RyR2_{Ser\text{-}2367\text{-}CFP/Tyr\text{-}2801\text{-}YFP}$ is capable of producing FRET, we determined its FRET efficiency by measuring the fluorescence intensity of CFP (donor) before and after bleaching YFP (acceptor) in live cells. As expected based on their close proximity in the three-dimensional structure of RyR2, HEK293 cells expressing $RyR2_{Ser\text{-}2367\text{-}CFP/Tyr\text{-}2801\text{-}YFP}$ displayed a significant level of FRET with a FRET efficiency of $14.4 \pm 1.1\%$ ($n = 20$) (Fig. 1*D*, *a* and *c*).

RyR is a homotetramer consisting of four identical subunits. It is possible that the FRET signal observed in $RyR2_{Ser\text{-}2367\text{-}CFP/Tyr\text{-}2801\text{-}YFP}$ results from the interaction between Ser-2367-CFP and Tyr-2801-YFP in the same RyR2 subunit (intra-subunit interaction) or between Ser-2367-CFP in one subunit and Tyr-2801-YFP in the neighboring subunit (inter-subunit interaction). To distinguish an intra-subunit from an inter-subunit interaction between the donor and acceptor in a FRET probe in tetramic RyRs, we have previously developed a co-expression approach (34). Using the same approach, we constructed RyR2 fusion proteins with a single insertion of Ser-2367-CFP ($RyR2_{Ser\text{-}2367\text{-}CFP}$) or a single insertion of Tyr-2801-YFP ($RyR2_{Tyr\text{-}2801\text{-}YFP}$) and co-expressed $RyR2_{Ser\text{-}2367\text{-}CFP}$ and $RyR2_{Tyr\text{-}2801\text{-}YFP}$ in HEK293 cells. Fig. 1*D* shows that, unlike cells transfected with $RyR2_{Ser\text{-}2367\text{-}CFP/Tyr\text{-}2801\text{-}YFP}$, HEK293 cells co-transfected with $RyR2_{Ser\text{-}2367\text{-}CFP}$ and $RyR2_{Tyr\text{-}2801\text{-}YFP}$ displayed no detectable FRET signals (Fig. 1*D*, *b* and *c*). In other words, there is no detectable interaction between Ser-2367-CFP of one subunit and Tyr-2801-YFP of the neighboring subunit, indicating that the FRET signal in $RyR2_{Ser\text{-}2367\text{-}CFP/Tyr\text{-}2801\text{-}YFP}$ results from intra-subunit interactions. Thus, collectively, our results indicate that Ser-2367-CFP/Tyr-2801-YFP pair is a functional, intra-subunit FRET probe.

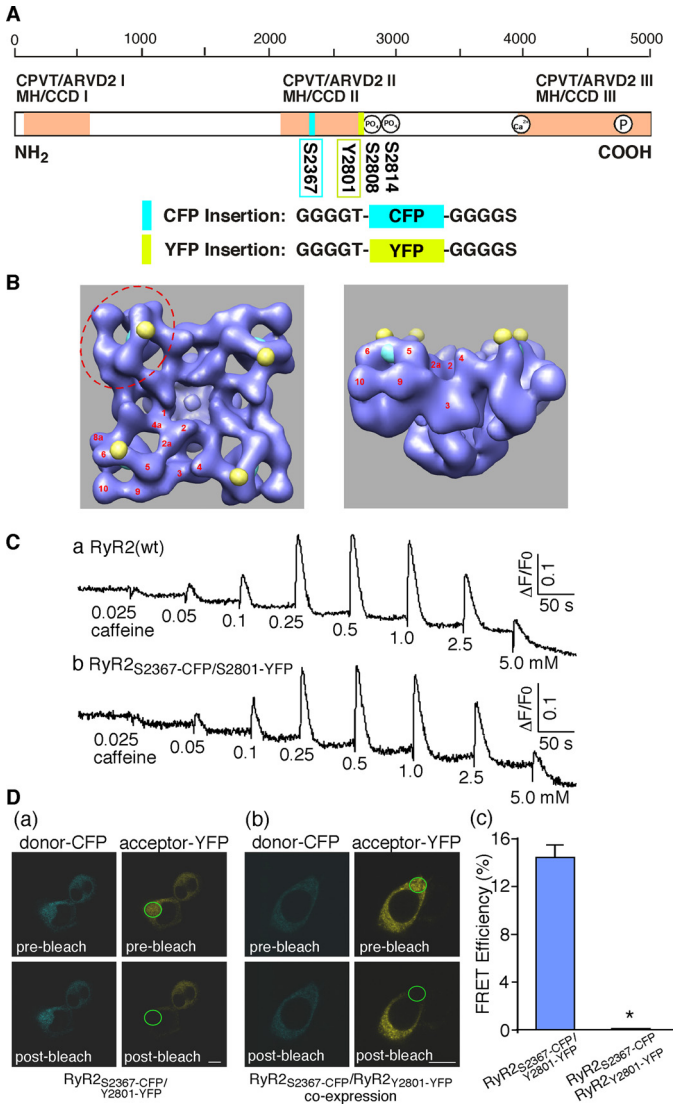

FIGURE 1. **Construction and characterization of a novel FRET pair Ser-2367-CFP/Tyr-2801-YFP in RyR2.** *A*, a schematic illustration of the linear sequence of RyR (*open box*) shows the three major hotspots (*pink boxes*) where disease-causing mutations frequently occur (*CPVT*, catecholaminergic polymorphic ventricular tachycardia; *ARVD2*, arrhythmogenic right ventricular dysplasia type 2; *MH*, malignant hyperthermia; *CCD*, central core disease). The locations of Ser-2367-CFP (*cyan box*), Tyr-2801-YFP (*yellow box*), the Ser-2808 and Ser-2814 phosphorylation sties, the cytosolic Ca^{2+} sensor, and the pore-forming segment (*circles inside the open box*) are also indicated. The inserted CFP and YFP are flanked by short glycine-rich linkers. *B*, shown are locations of Ser-2367-CFP (*cyan spheres*) and Tyr-2801-YFP (*yellow spheres*) in the three-dimensional architecture of RyR (*left*, *top view*; *right*, *side view*) based on the previous three-dimensional reconstructions of the $RyR2_{Ser\text{-}2367\text{-}GFP}$ and $RyR2_{Tyr\text{-}2801\text{-}GFP}$ fusion proteins (21, 23). The distance between CFP and YFP is 30 Å. The clamp region (*red dashed ellipse*) and subdomains (*red numbers*) are indicated. *C*, Caffeine induced Ca^{2+} release in HEK293 cells transfected with RyR2(wt) (*a*) or $RyR2_{Ser\text{-}2367\text{-}CFP/Tyr\text{-}2801\text{-}YFP}$ (*b*). Transfected HEK293 cells were loaded with fluo-3 AM. The fluorescence intensity of the fluo-3-loaded cells was monitored continuously before and after the sequential additions of increasing concentrations of caffeine (0.025 to 5 mM). *D*, confocal images show cyan fluorescence of the donor CFP and yellow fluorescence of the acceptor YFP before (*top panels*) and after (*bottom panels*) photobleaching of a small area (indicated by a *green ellipse*) in HEK239 cells transfected with $RyR2_{Ser\text{-}2367\text{-}CFP/Tyr\text{-}2801\text{-}YFP}$ (*a*) or co-transfected with $RyR2_{Ser\text{-}2367\text{-}CFP}$ and $RyR2_{Tyr\text{-}2801\text{-}YFP}$ (*b*) and the corresponding FRET efficiencies (*c*). The *scale bar* represents 10 μm. Data shown are the mean ± S.E. ($n = 20$). *, $p < 0.01$.

The Ser-2367-CFP/Tyr-2801-YFP FRET Probe Is a Dynamic, Functional Conformation Sensor

We next determined whether this intra-subunit FRET probe (Ser-2367-CFP/Tyr-2801-YFP) is capable of sensing conformational changes in RyR2. We activated $RyR2_{Ser\text{-}2367\text{-}CFP/Tyr\text{-}2801\text{-}YFP}$ with various concentrations of caffeine to alter the conformational and functional state of the channel and continuously monitored the FRET signal by determining the fluorescence ratio of YFP and CFP upon CFP excitation. We reasoned that if caffeine activation of RyR2 leads to conformational changes in the clamp region, it would alter the relative positions of Ser-2367-CFP and Tyr-2801-YFP and thus their FRET signals. Indeed, as shown in Fig. 2*A*, caffeine reduced the FRET signal in HEK293 cells expressing $RyR2_{Ser\text{-}2367\text{-}CFP/Tyr\text{-}2801\text{-}YFP}$ in a concentration-dependent manner. The effect of caffeine on FRET is reversible. Upon caffeine wash-off, the FRET signal recovered to a level similar to that before caffeine treatment.

To assess whether caffeine-induced FRET changes are associated with functional changes, we monitored caffeine-induced Ca^{2+} release in HEK293 cells by determining the ER luminal Ca^{2+} level using a FRET-based ER luminal Ca^{2+} sensor, D1ER. We have previously shown that caffeine reduces the ER luminal Ca^{2+} level at which spontaneous Ca^{2+} release occurs (*i.e.* the threshold for spontaneous store-overload-induced Ca^{2+} release (SOICR)) (33, 40–42). The threshold for SOICR reflects the propensity (or functional state) of the RyR2 channel for spontaneous Ca^{2+} release (40, 41). As shown in Fig. 2, we found that caffeine concentration dependently and reversibly reduced the SOICR threshold in HEK293 cells expressing $RyR2_{Ser\text{-}2367\text{-}CFP/Tyr\text{-}2801\text{-}YFP}$ (Fig. 2*B*) and RyR2(wt) (Fig. 2*C*) to a similar extent (Fig. 2*D*). Note that the CFP or YFP fluorescence intensity in HEK293 cells expressing $RyR2_{Ser\text{-}2367\text{-}CFP/Tyr\text{-}2801\text{-}YFP}$ alone is only ~10% that in cells expressing both D1ER and $RyR2_{Ser\text{-}2367\text{-}CFP/Tyr\text{-}2801\text{-}YFP}$ (data not shown). Thus, the FRET signal detected in cells expressing both D1ER and $RyR2_{Ser\text{-}2367\text{-}CFP/Tyr\text{-}2801\text{-}YFP}$ largely reflects that of the D1ER luminal Ca^{2+} sensor. Taken together, these data indicate that the concentration dependence of caffeine-induced FRET changes is similar to that of caffeine-induced changes in the SOICR threshold (Fig. 2*D*). Hence, caffeine-induced FRET changes closely correlate with the functional states of the channel.

To ascertain whether the large N-terminal cytosolic domain of RyR2 itself is sufficient to confer FRET between Ser-2367-CFP and Tyr-2801-YFP and its response to caffeine, we determined the FRET efficiency of a C-terminal-truncated RyR2 containing the same Ser-2367-CFP/Tyr-2801-YFP FRET pair, $RyR2\text{-}(1–4770)_{Ser\text{-}2367\text{-}CFP/Tyr\text{-}2801\text{-}YFP}$ (a channel lacking the small pore-forming domain) (30). We found that $RyR2\text{-}(1–4770)_{Ser\text{-}2367\text{-}CFP/Tyr\text{-}2801\text{-}YFP}$ still exhibited significant FRET (Fig. 2*E*). However, caffeine did not change the FRET efficiency of $RyR2\text{-}(1–4770)_{Ser\text{-}2367\text{-}CFP/Tyr\text{-}2801\text{-}YFP}$, whereas caffeine reduced the FRET efficiency of $RyR2_{Ser\text{-}2367\text{-}CFP/Tyr\text{-}2801\text{-}YFP}$ in a concentration-dependent manner (Fig. 2*E*). Thus, the large N-terminal domain of RyR2 itself is not sufficient for caffeine-induced conformational changes in the clamp region. It should be noted that caffeine does not affect the fluores-

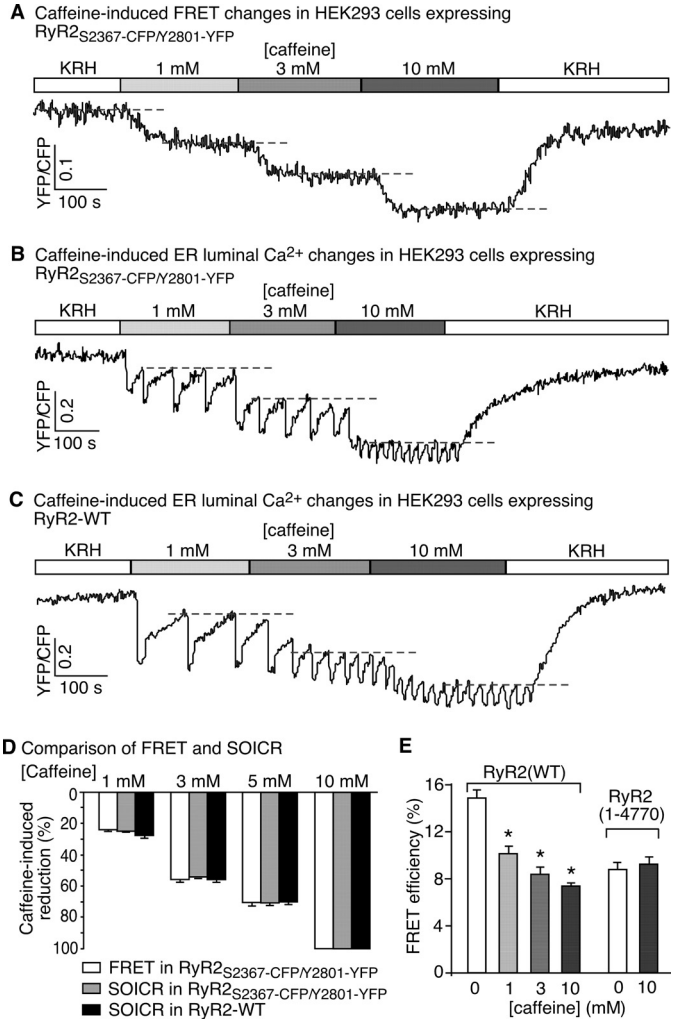

FIGURE 2. **Caffeine induces correlated structural and functional changes in RyR2.** *A*, stable, inducible HEK293 cells expressing $RyR2_{Ser\text{-}2367\text{-}CFP/Tyr\text{-}2801\text{-}YFP}$ were perfused with KRH buffer containing increasing levels of caffeine (0–10 mM) to induce conformational changes in RyR2. A representative recording of the Ser-2367-CFP/Tyr-2801-YFP FRET signal from a single HEK293 cell is shown. Changes in the Ser-2367-CFP/Tyr-2801-YFP FRET signal reflect structural changes in the clamp region of RyR2. *Dashed lines* indicate steady-state FRET levels at different concentrations of caffeine. *B*, stable, inducible HEK293 cells expressing $RyR2_{Ser\text{-}2367\text{-}CFP/Tyr\text{-}2801\text{-}YFP}$ were transfected with the FRET-based ER luminal Ca^{2+}-sensing protein, D1ER. The transfected cells were perfused with KRH buffer containing increasing levels of caffeine (0–10 mM). The trace shows a representative FRET recording from a single HEK293 cell expressing both D1ER and $RyR2_{Ser\text{-}2367\text{-}CFP/Tyr\text{-}2801\text{-}YFP}$. Because the CFP or YFP fluorescence intensity in HEK293 cells expressing $RyR2_{Ser\text{-}2367\text{-}CFP/Tyr\text{-}2801\text{-}YFP}$ alone is only ~10% that in cells expressing both the D1ER luminal Ca^{2+} sensor and $RyR2_{Ser\text{-}2367\text{-}CFP/Tyr\text{-}2801\text{-}YFP}$, the FRET signals detected largely came from those of D1ER. These D1ER FRET signals reflect the ER luminal Ca^{2+} levels. *Dashed lines* indicate the ER luminal Ca^{2+} levels at which SOICR occurs (*i.e.* the SOICR threshold), which reflects the functional state of RyR2. *C*, single cell D1ER FRET imaging of stable, inducible, RyR2(wt)-expressing HEK293 cells were transfected with D1ER at increasing levels of caffeine. *Dashed lines* indicate SOICR thresholds. *D*, comparison of caffeine-induced, concentration-dependent changes in the Ser-2367-CFP/Tyr-2801-YFP FRET signal (structural changes) with those in the SOICR threshold (functional changes). The extents of changes in FRET and SOICR at each caffeine concentration were normalized to those at 10 mM caffeine (100%). Data shown are the mean ± S.E. (n = 4–11). There are no significant differences between reductions in FRET and SOICR threshold under each condition. *E*, the FRET efficiency in HEK293 cells expressing $RyR2_{Ser\text{-}2367\text{-}CFP/Tyr\text{-}2801\text{-}YFP}$ or a truncated RyR2, $RyR2\text{-}(1–4770)_{Ser\text{-}2367\text{-}CFP/Tyr\text{-}2801\text{-}YFP}$, at various caffeine concentrations (0–10 mM) was determined using the photobleaching method. Data shown are the mean ± S.E. (n = 30) (*, $p < 0.05$; *versus* 0 mM caffeine).

cence intensity of HEK293 cells transfected with $RyR2_{Ser\text{-}2367\text{-}CFP}$ or $RyR2_{Tyr\text{-}2801\text{-}YFP}$ alone or co-transfected with $RyR2_{Ser\text{-}2367\text{-}CFP}$ and $RyR2_{Tyr\text{-}2801\text{-}YFP}$ (data not shown). The results of these control experiments indicate that caffeine-induced FRET changes in HEK293 cells expressing $RyR2_{Ser\text{-}2367\text{-}CFP/Tyr\text{-}2801\text{-}YFP}$ did not result from a direct effect of caffeine on the fluorescence of CFP or YFP. Taken together, these data indicate that the Ser-2367-CFP/Tyr-2801-YFP FRET probe is capable of sensing functionally correlated conformational changes in the clamp region of RyR2.

Ligand-dependent Conformational Changes in the Clamp Region of RyR2

A number of pharmacological and physiological ligands can activate RyR2, leading to Ca^{2+} release, but the molecular mechanisms of their activation are largely unknown. In the next series of experiments we took advantage of our newly constructed conformation sensor to study the conformational changes in the clamp region of RyR2 activated by various ligands.

Aminophylline, Theophylline, and 4-CmC—In addition to caffeine, other pharmacological ligands, such as aminophylline, theophylline, and 4-CmC, have been shown to activate RyR2 and induce sarcoplasmic reticulum Ca^{2+} release (42–44). To determine whether different pharmacological ligands may have different effects on RyR2 conformation, we assessed the impact of aminophylline, theophylline and 4-CmC on FRET and the ER luminal Ca^{2+} level in HEK293 cells expressing $RyR2_{Ser\text{-}2367\text{-}CFP/Tyr\text{-}2801\text{-}YFP}$. Fig. 3 shows that, like caffeine, aminophylline and theophylline reduced both the FRET level and the SOICR threshold, indicating that these two RyR2 agonists induce Ca^{2+} release and conformational changes in the clamp region (Fig. 3, *A*, *B*, and *E*). Interestingly, we found that 4-CmC did not cause any significant changes in the FRET signal, but it induced Ca^{2+} release (Fig. 3, *C*, *D*, and *E*).

ATP and Ca^{2+}—ATP and Ca^{2+} are two physiological agonists of RyR2 (3). To assess the effect of cytosolic ATP and Ca^{2+} on the conformation and function of RyR2, we perfused permeabilized HEK293 cells expressing $RyR2_{Ser\text{-}2367\text{-}CFP/Tyr\text{-}2801\text{-}YFP}$ with an ICM or with ICM plus 5 mM ATP or 1 μM Ca^{2+}. As shown in Fig. 4, ATP reversibly reduced both the FRET signal and the SOICR threshold (Fig. 4, *A*, *B*, and *E*), indicating that, like caffeine, ATP is able to induce conformational changes in the clamp region and concomitant intracellular Ca^{2+} release. Surprisingly, elevating cytosolic Ca^{2+} to 1 μM induced little or no FRET changes in the $RyR2_{Ser\text{-}2367\text{-}CFP/Tyr\text{-}2801\text{-}YFP}$-expressing cells, but it did reduce the SOICR threshold (Fig. 4, *C*, *D*, and *E*). Further elevation of cytosolic Ca^{2+} to 10 μM did not induce significant changes in FRET (1.93 ± 1.20% of that induced by 10 mM caffeine, $n = 4$). Thus, unlike caffeine and ATP, cytosolic Ca^{2+} activates the RyR2 channel without inducing major conformational changes in the clamp region. Furthermore, we determined the impact of ATP, Ca^{2+}, and 4-CmC on the FRET efficiency in HEK293 cells expressing $RyR2_{Ser\text{-}2367\text{-}CFP/Tyr\text{-}2801\text{-}YFP}$. Similarly, we found that ATP reduced the FRET efficiency, whereas Ca^{2+} and 4-CmC had no effect on the FRET efficiency (Fig. 4*F*). Taken together, these observations indicate that the activation of RyR2 by caffeine, aminophylline, theophylline, and ATP is associated with substantial conformational changes

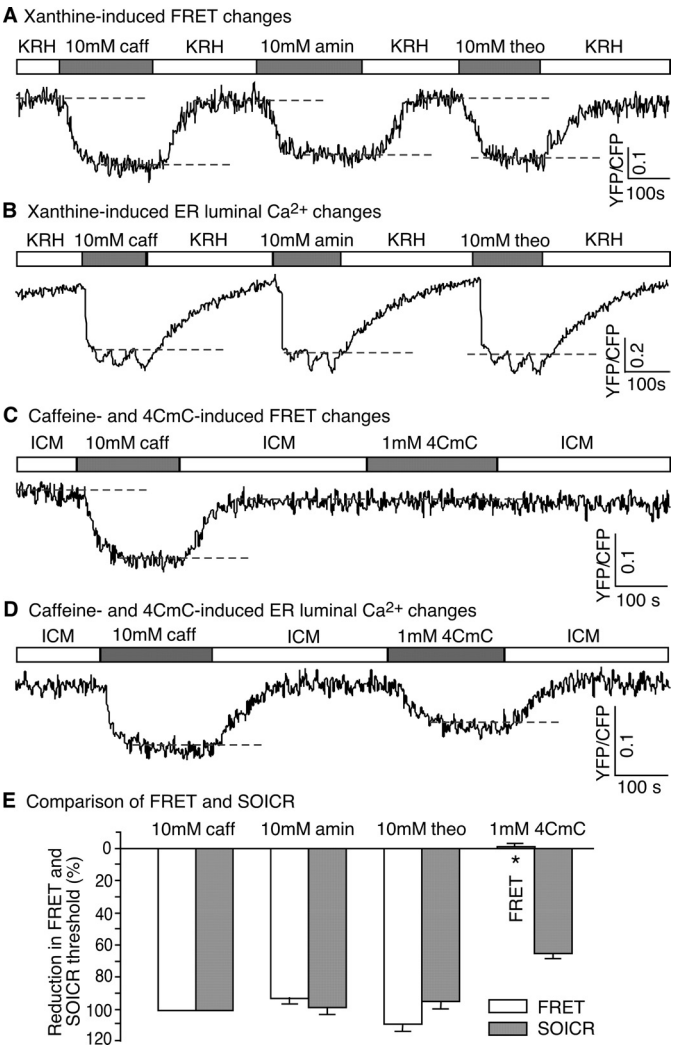

FIGURE 3. **Effect of aminophylline, theophylline, and 4-CmC on the structure and function of RyR2.** *A*, HEK293 cells expressing $RyR2_{Ser\text{-}2367\text{-}CFP/Tyr\text{-}2801\text{-}YFP}$ were perfused with KRH buffer without or with caffeine (10 mM), aminophylline (10 mM), or theophylline (10 mM). A representative single cell recording of the Ser-2367-CFP/Tyr-2801-YFP FRET signal is shown. *Dashed lines* indicate steady-state FRET levels. *B*, shown is a representative single cell luminal Ca^{2+} recording of D1ER-transfected HEK293 cells expressing $RyR2_{Ser\text{-}2367\text{-}CFP/Tyr\text{-}2801\text{-}YFP}$ in the KRH buffer without or with caffeine, aminophylline, or theophylline. *Dashed lines* indicate the SOICR threshold. *C*, HEK293 cells expressing $RyR2_{Ser\text{-}2367\text{-}CFP/Tyr\text{-}2801\text{-}YFP}$ were permeabilized and perfused with the ICM buffer without or with caffeine (10 mM) or 4-CmC (1 mM). A representative single cell recording of the Ser-2367-CFP/Tyr-2801-YFP FRET signal is shown. *D*, a representative single cell luminal Ca^{2+} recording of D1ER-transfected, permeabilized HEK293 cells expressing $RyR2_{Ser\text{-}2367\text{-}CFP/Tyr\text{-}2801\text{-}YFP}$ in ICM without or with caffeine or 4-CmC. *Dashed lines* indicate the SOICR threshold. *E*, shown is a comparison of changes in the Ser-2367-CFP/Tyr-2801-YFP FRET signal (structural changes) with those in the SOICR threshold (functional changes) induced by caffeine, aminophylline, theophylline, or 4-CmC. The extents of changes in FRET and SOICR were normalized to those at 10 mM caffeine (100%). Data shown are the mean ± S.E. ($n = 5$–11) (*, $p < 0.01$; FRET *versus* SOICR).

in the clamp region of RyR2, whereas the activation of RyR2 by cytosolic Ca^{2+} and 4-CmC is not. Thus, different ligands activate RyR2 and induce Ca^{2+} release by different mechanisms associated with distinct conformational changes.

Ryanodine Keeps the Channel Open but Does Not Lock RyR in a Fixed Conformation

It is well known that ryanodine binds to the open state of RyR and keeps the channel in an open, subconductance state (5, 6,

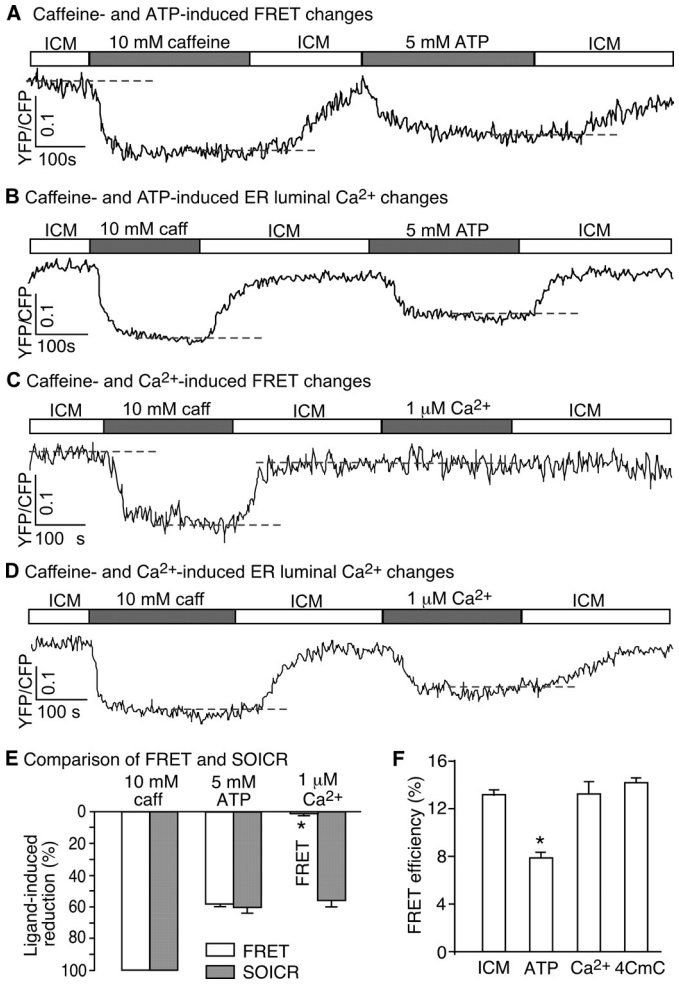

FIGURE 4. **Differential effects of cytosolic ATP and Ca^{2+} on the conformational dynamics of RyR2.** *A*, HEK293 cells expressing $RyR2_{Ser\text{-}2367\text{-}CFP/Tyr\text{-}2801\text{-}YFP}$ were permeabilized and perfused with ICM without or with caffeine (10 mM) or ATP (5 mM). A representative single cell recording of the Ser-2367-CFP/Tyr-2801-YFP FRET signal is shown. *B*, shown is a representative single cell luminal Ca^{2+} recording of D1ER-transfected, permeabilized HEK293 cells expressing $RyR2_{Ser\text{-}2367\text{-}CFP/Tyr\text{-}2801\text{-}YFP}$ in the ICM buffer with or without caffeine or ATP. The SOICR threshold is indicated by a *dashed line*. *C*, HEK293 cells expressing $RyR2_{Ser\text{-}2367\text{-}CFP/Tyr\text{-}2801\text{-}YFP}$ were permeabilized and perfused with ICM without or with caffeine (10 mM) or Ca^{2+} (1 μM). A representative single cell recording of the Ser-2367-CFP/Tyr-2801-YFP FRET signal is shown. Note that unlike ATP, Ca^{2+} induced no changes in FRET. *D*, a representative single cell luminal Ca^{2+} recording of D1ER-transfected, permeabilized HEK293 cells expressing $RyR2_{Ser\text{-}2367\text{-}CFP/Tyr\text{-}2801\text{-}YFP}$ in the ICM buffer without or with caffeine or Ca^{2+} is shown. The *dashed line* indicates the SOICR threshold. *E*, shown is a comparison of changes in the Ser-2367-CFP/Tyr-2801-YFP FRET signal (structural changes) with those in the SOICR threshold (functional changes) induced by caffeine, ATP, or Ca^{2+}. The extents of changes in FRET and SOICR were normalized to those at 10 mM caffeine (100%). Data shown are the mean ± S.E. (n = 7–14) (*, $p < 0.01$; FRET *versus* SOICR). *F*, shown is FRET efficiency in permeabilized HEK293 cells expressing $RyR2_{Ser\text{-}2367\text{-}CFP/Tyr\text{-}2801\text{-}YFP}$ in ICM without or with ATP, Ca^{2+}, or 4-CmC. Data shown are the mean ± S.E. (n = 20–30). *, $p < 0.01$; *versus* ICM.

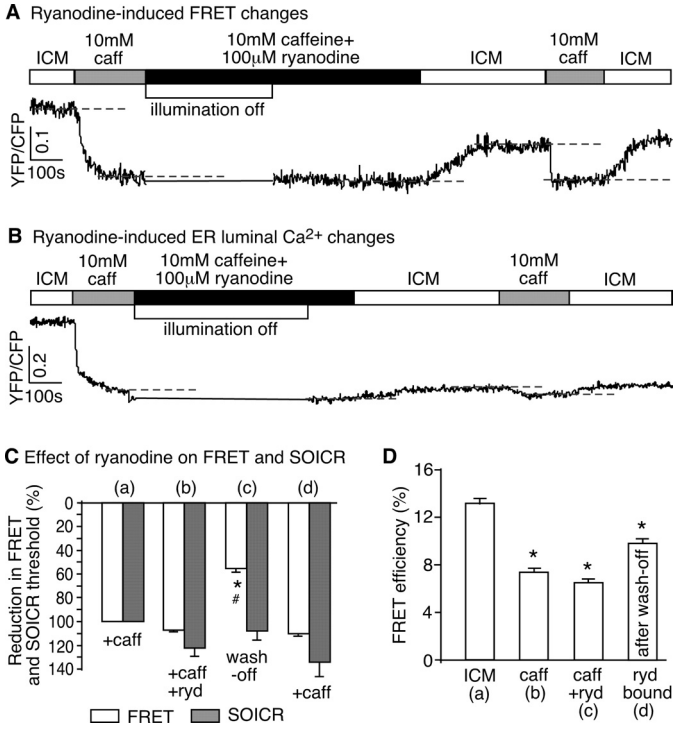

FIGURE 5. **Impact of ryanodine on the structure and function of RyR2.** *A*, HEK293 cells transfected with $RyR2_{Ser\text{-}2367\text{-}CFP/Tyr\text{-}2801\text{-}YFP}$ were permeabilized and perfused with ICM, caffeine (10 mM), and caffeine (10 mM) plus ryanodine (100 μM) followed by wash-off with ICM. The cells were then perfused with caffeine (10 mM) again followed by wash-off with ICM. The illumination was turned off during part of the long incubation with caffeine plus ryanodine to minimize photobleaching. A representative single cell recording of the Ser-2367-CFP/Tyr-2801-YFP FRET signal is shown. *B*, shown is a representative single cell luminal Ca^{2+} recording of D1ER-transfected, permeabilized HEK293 cells expressing $RyR2_{Ser\text{-}2367\text{-}CFP/Tyr\text{-}2801\text{-}YFP}$. The cells were perfused in the same way as that described in *panel A*. Note that the ER Ca^{2+} store remained depleted after the addition of ryanodine. *C*, shown is a comparison of the changes in the Ser-2367-CFP/Tyr-2801-YFP FRET signal and those in the SOICR threshold under various conditions: *a*, caffeine (10 mM) (control); *b*, caffeine (10 mM) plus ryanodine (100 μM), *c*, after wash-off; *d*, re-application of caffeine (10 mM). The extents of changes in FRET and SOICR threshold were normalized to those in the control (100%). Data shown are the mean ± S.E. (n = 4–8). *, $p < 0.01$; FRET *versus* SOICR; #, $p < 0.01$ *versus* before or after caffeine treatment. *D*, HEK293 cells expressing $RyR2_{Ser\text{-}2367\text{-}CFP/Tyr\text{-}2801\text{-}YFP}$ were permeabilized and perfused with ICM (*a*), caffeine (10 mM) (*b*), caffeine (10 mM) plus ryanodine (100 μM) (*c*) followed by wash-off (*d*). The FRET efficiency under each of these conditions was determined by the photobleaching method. Data shown are the mean ± S.E. (n = 30). *, $p < 0.01$; *versus* ICM.

45, 46). It is unclear, however, whether ryanodine locks RyR in a fixed conformation. To address this question, we determined whether caffeine could still induce conformational changes in a ryanodine-bound channel. To this end we first perfused the permeabilized HEK293 cells expressing $RyR2_{Ser\text{-}2367\text{-}CFP/Tyr\text{-}2801\text{-}YFP}$ with caffeine (10 mM) to open the channel and then with caffeine (10 mM) plus ryanodine (100 μM) to allow ryanodine binding to the caffeine-opened channels. These caffeine and ryanodine-treated cells were then perfused with the ICM buffer to remove caffeine and unbound ryanodine in order to reveal the effect of bound ryanodine, which is known to remain bound to RyR2. As shown in Fig. 5 *A*, caffeine reduced the FRET signal. Caffeine plus ryanodine caused a small further reduction in FRET. After removing caffeine and unbound ryanodine, the FRET signal recovered partially to a level that is significantly lower than the FRET level before caffeine treatment (Fig. 5*C*). To confirm that ryanodine remained bound to RyR2 after wash-off with the ICM buffer, we performed [^{3}H]ryanodine binding (see "Experimental Procedures"). We found that the amount of [^{3}H]ryanodine binding to cells pretreated with 100 μM non-labeled ryanodine plus 10 mM caffeine is only 1.21 ± 0.08% (mean ± S.E., n = 3) that of control cells without ryanodine pretreatment. Thus, most of the RyR2 channels were bound with ryanodine after pretreatment with 100 μM ryanodine plus 10 mM caffeine and remained bound with it after wash-off with the ICM buffer.

Therefore, the reduced FRET signal detected after wash-off with ICM (Fig. 5*C*) likely reflects the ryanodine-induced conformational changes in the ryanodine-bound channels. We also determined the FRET efficiencies in permeabilized $RyR2_{Ser\text{-}2367\text{-}CFP/Tyr\text{-}2801\text{-}YFP}$-expressing cells in the absence or presence of caffeine or ryanodine or after wash-off (Fig. 5*D*). Similarly, we found that caffeine or caffeine plus ryanodine reduced the FRET efficiency to a similar extent and that the FRET efficiency after removing caffeine and unbound ryanodine is lower than that before caffeine treatment (Fig. 5*D*). These data indicate that the bound ryanodine reduced the FRET signal or caused conformational changes in the clamp region but to a lesser extent than caffeine (10 mM). Importantly, a subsequent addition of caffeine to the ryanodine-treated cells could still reduce the FRET signal (Fig. 5, *A* and *C*). Thus, caffeine is still able to induce conformational changes in the ryanodine-bound RyR2 channel.

The impact of caffeine and ryanodine on RyR2 function is shown in Fig. 5*B*. Consistent with their known actions, caffeine caused store Ca^{2+} depletion. The addition of ryanodine in the presence of caffeine caused a small further reduction in store Ca^{2+} (Fig. 5*B*). The store Ca^{2+} level remained depleted after removing caffeine and unbound ryanodine (Fig. 5, *B* and *C*). These observations are in agreement with the view that ryanodine interacts with the caffeine-opened RyR2 and keeps the channel in the open state, leading to store Ca^{2+} depletion. Taken together, these results indicate that ryanodine induces conformational changes in the clamp region of RyR2 and that the ryanodine-induced conformation can still be altered by caffeine.

DISCUSSION

RyR represents the largest known ion channel being composed of four identical subunits with a molecular mass of ~2.3 MDa (3). Its gigantic three-dimensional structure consists of a large cytoplasmic assembly and a smaller transmembrane domain (47–49). It has long been appreciated that global conformational changes are involved in the gating and regulation of the RyR channel (12–17). Abnormal conformational changes in RyR are believed to underlie a common cause of RyR-associated diseases (16, 50, 51). However, the molecular basis of conformational changes in RyR remains incompletely understood. In the present study, we built a FRET-based probe to assess the conformational changes in the corner region of the large square-shaped cytoplasmic assembly, also known as the clamp region, of the three-dimensional architecture of RyR2 (14, 15, 19). Using this novel conformation sensor, we demonstrate for the first time that ligand-induced Ca^{2+} release via activation of RyR2 is not always correlated with conformational changes in the clamp region, suggesting the existence of multiple mechanisms of RyR2 activation associated with unique conformational changes.

Ligand-dependent Conformational Changes in RyR—Substantial structural rearrangements in the clamp region of the three-dimensional architecture of RyR occur upon channel activation by an ATP analog, AMP-PCP, or ryanodine in the presence of high concentrations of Ca^{2+} (100 μM) (14, 15, 18, 19). Interestingly, Ca^{2+} alone did not appear to cause significant conformational changes in the clamp region (15). Consistent with these cryo-EM findings, we also detected conformational changes in the clamp region induced by ATP and ryanodine but not by Ca^{2+} alone using our novel FRET-based conformation probe, confirming the utility and sensitivity of our FRET approach. However, the reason for the different effect of Ca^{2+} is unclear. It was suggested that the three-dimensional reconstruction of RyR in the presence of Ca^{2+} alone represents the average of a channel population with both the open and closed states as Ca^{2+} alone only transiently activates the channel. On the other hand, the reconstruction of RyR in the presence of AMP-PCP/Ca^{2+} or ryanodine/Ca^{2+} represents mainly the open state as these ligands fully activated the channel. However, although Ca^{2+} alone produced little conformational changes in the clamp region, it induced structural rearrangements in the transmembrane domain of RyR to an extent similar to that observed with AMP-PCP/Ca^{2+} (15). Thus, these observations raise a possibility that conformational changes in the clamp region may be ligand-dependent.

Recently, a higher resolution (~10 Å) three-dimensional reconstruction of RyR has been obtained in the presence of a potent RyR agonist, PCB 95 together with Ca^{2+} (50 μM) and FKBP12.6 (17). Substantial differences in the clamp and central regions in the cytoplasmic assembly and in the transmembrane domain of RyR were noticed when comparing the three-dimensional reconstruction in the presence of PCB 95/Ca^{2+} with intermediate resolution (~30 Å) three-dimensional reconstruction in the presence of AMP-PCP/Ca^{2+} or ryanodine/Ca^{2+} (14, 15). These differences were thought to be due to the low resolution of the early three-dimensional reconstructions. Alternatively, it is possible that PCB 95/Ca^{2+}/FKBP12.6 may induce different conformational changes in RyR compared with AMP-PCP/Ca^{2+} or ryanodine/Ca^{2+}.

To further assess the ligand dependence of conformational changes in the clamp region, we used our FRET probe to monitor the conformational changes in the clamp region of RyR upon binding to various ligands. These ligand-induced conformational changes were then correlated with the functional state of the channel in the presence of the same ligand. We found that caffeine, aminophylline, theophylline, ATP, and ryanodine induced conformational changes in the clamp region and concomitant Ca^{2+} release, whereas Ca^{2+} and 4-CmC induced Ca^{2+} release in a manner compatible to that induced by caffeine and ATP but caused no detectable conformational changes in the clamp region. Thus, different from caffeine, ATP, and ryanodine, Ca^{2+}, and 4-CmC activate RyR and Ca^{2+} release without inducing significant conformational changes in the clamp region.

Using a different FRET probe designed to monitor the conformational changes between the N-terminal domain and the central disease mutation hotspot of RyR2, we have previously shown that caffeine increased the FRET signal, whereas ATP and 4-CmC reduced it (34). On the other hand, in the present study we found that both caffeine and ATP decreased the FRET signal of the clamp FRET probe, whereas 4-CmC showed no effect. These studies using two different FRET probes indicate that the conformational changes induced by caffeine, ATP, or 4-CmC are different. Taken together, our FRET analysis and

cryo-EM reconstructions demonstrate that conformational changes in RyR are ligand-dependent and suggest that different ligands may activate the RyR channel via different mechanisms with distinct conformational changes.

Functional and Structural Impact of Ryanodine on RyR—It is widely believed that ryanodine locks the RyR channel into an open, subconductance state and that the ryanodine-modified channel is insensitive to further modulation by other channel ligands (5, 6, 45, 46). In contrast, it has been shown that ryanodine increases the sensitivity of single RyR2 channels to cytosolic Ca^{2+} activation by ~1000-fold and that single ryanodine-modified RyR2 channels remain sensitive to modulation by channel modulators such as Mg^{2+} and caffeine (52, 53). Thus, functionally, ryanodine does not lock the RyR channel into an open state. Instead, ryanodine dramatically sensitizes the channel to cytosolic Ca^{2+} activation. However, it is unclear whether, structurally, ryanodine locks the channel in a fixed conformational state. To address this question, we monitored the impact of caffeine on conformational changes in the clamp region of RyR2 before and after ryanodine modification. We found that ryanodine, upon binding, kept the channel open and induced conformational changes in the clamp region, which is consistent with the structural rearrangements in the three-dimensional architecture of ryanodine-modified RyR observed by cryo-EM (14). Importantly, we found that caffeine still induced further conformational changes in the clamp region of ryanodine-modified RyR2 channels. These data indicate that although ryanodine may keep the channel fully open by markedly sensitizing it to Ca^{2+} activation, it does not lock the receptor conformation into a fixed state.

Generation of Domain-specific FRET Probes for Studying Conformational Changes in RyR—Cryo-EM and three-dimensional reconstructions have provided important information on the structural domains or regions that undergo conformational changes in RyR upon ligand binding. However, because of the relatively low resolutions of current three-dimensional reconstructions, the amino acid sequences that are involved in ligand-induced conformational changes in RyR have yet to be determined. Furthermore, little is known about the dynamics, ligand dependence or functional correlations of these conformational changes. An alternative approach to studying conformational changes is the use of domain specific FRET-based probes. Using GFP as a structural marker, we have previously mapped a number of specific sites or sequences onto the three-dimensional structure of RyR (21–23, 36–39). The docking of crystal structures of RyR fragments into the cryo-EM density map of RyR has also led to the sequence assignment of some specific domains (20, 50, 51). These sequence-structure correlations allow us to design and build FRET-based probes in specific domains or regions of the RyR structure. Using this approach, we have previously constructed a FRET probe for monitoring the conformational dynamics involving the N-terminal and central regions of RyR2 (34). In the present study, we built a FRET probe for studying the ligand dependence and functional correlation of the conformational dynamics in the clamp region. Hence, domain-specific FRET probes are an effective approach for monitoring conformational changes in RyR. Generation of a network of domain-specific FRET probes should allow us to systematically and comprehensively study the conformational dynamics and ligand gating mechanisms of RyR.

Acknowledgment—We gratefully acknowledge the Advanced Light Microscopy and Image Analysis Core Facilities at the Wadsworth Center.

REFERENCES

1. Bers, D. M. (2002) Cardiac excitation-contraction coupling. *Nature* **415,** 198–205
2. Berridge, M. J., Bootman, M. D., and Roderick, H. L. (2003) Calcium signaling. Dynamics, homeostasis, and remodelling. *Nat. Rev. Mol. Cell Biol.* **4,** 517–529
3. Fill, M., and Copello, J. A. (2002) Ryanodine receptor calcium release channels. *Physiol. Rev.* **82,** 893–922
4. Meissner, G. (2004) Molecular regulation of cardiac ryanodine receptor ion channel. *Cell Calcium* **35,** 621–628
5. Zucchi, R., and Ronca-Testoni, S. (1997) The sarcoplasmic reticulum Ca^{2+} channel/ryanodine receptor. Modulation by endogenous effectors, drugs, and disease states. *Pharmacol. Rev.* **49,** 1–51
6. Xu, L., Tripathy, A., Pasek, D. A., and Meissner, G. (1998) Potential for pharmacology of ryanodine receptor/calcium release channels. *Ann. N.Y. Acad. Sci.* **853,** 130–148
7. Eisner, D. A., Díaz, M. E., O'Neill, S. C., and Trafford, A. W. (2004) Physiological and pathological modulation of ryanodine receptor function in cardiac muscle. *Cell Calcium* **35,** 583–589
8. Eisner, D. A., Kashimura, T., Venetucci, L. A., and Trafford, A. W. (2009) From the ryanodine receptor to cardiac arrhythmias. *Circ. J.* **73,** 1561–1567
9. Capes, E. M., Loaiza, R., and Valdivia, H. H. (2011) Ryanodine receptors. *Skelet. Muscle* **1,** 18
10. Priori, S. G., and Chen, S. R. (2011) Inherited dysfunction of sarcoplasmic reticulum Ca^{2+} handling and arrhythmogenesis. *Circ. Res.* **108,** 871–883
11. Maclennan, D. H., and Zvaritch, E. (2011) Mechanistic models for muscle diseases and disorders originating in the sarcoplasmic reticulum. *Biochim. Biophys. Acta* **1813,** 948–964
12. Ohkusa, T., Kang, J. J., Morii, M., and Ikemoto, N. (1991) Conformational change of the foot protein of sarcoplasmic reticulum as an initial event of calcium release. *J. Biochem.* **109,** 609–615
13. el-Hayek, R., Yano, M., and Ikemoto, N. (1995) A conformational change in the junctional foot protein is involved in the regulation of Ca^{2+} release from sarcoplasmic reticulum. Studies on polylysine-induced Ca^{2+} release. *J. Biol. Chem.* **270,** 15634–15638
14. Orlova, E. V., Serysheva, I. I., van Heel, M., Hamilton, S. L., and Chiu, W. (1996) Two structural configurations of the skeletal muscle calcium release channel. *Nat. Struct. Biol.* **3,** 547–552
15. Serysheva, I. I., Schatz, M., van Heel, M., Chiu, W., and Hamilton, S. L. (1999) Structure of the skeletal muscle calcium release channel activated with Ca^{2+} and AMP-PCP. *Biophys. J.* **77,** 1936–1944
16. Ikemoto, N., and Yamamoto, T. (2002) Regulation of calcium release by interdomain interaction within ryanodine receptors. *Front. Biosci.* **7,** d671–d683
17. Samsó, M., Feng, W., Pessah, I. N., and Allen, P. D. (2009) Coordinated movement of cytoplasmic and transmembrane domains of RyR1 upon gating. *PLoS Biol.* **7,** e85
18. Sharma, M. R., Jeyakumar, L. H., Fleischer, S., and Wagenknecht, T. (2000) Three-dimensional structure of ryanodine receptor isoform three in two conformational states as visualized by cryo-electron microscopy. *J. Biol. Chem.* **275,** 9485–9491
19. Sharma, M. R., Jeyakumar, L. H., Fleischer, S., and Wagenknecht, T. (2006) Three-dimensional visualization of FKBP12.6 binding to an open conformation of cardiac ryanodine receptor. *Biophys. J.* **90,** 164–172
20. Yuchi, Z., Lau, K., and Van Petegem, F. (2012) Disease mutations in the ryanodine receptor central region. Crystal structures of a phosphorylation hot spot domain. *Structure* **20,** 1201–1211

21. Meng, X., Xiao, B., Cai, S., Huang, X., Li, F., Bolstad, J., Trujillo, R., Airey, J., Chen, S. R., Wagenknecht, T., and Liu, Z. (2007) Three-dimensional localization of serine 2808, a phosphorylation site in cardiac ryanodine receptor. *J. Biol. Chem.* **282,** 25929–25939
22. Liu, Z., Zhang, J., Wang, R., Wayne Chen, S. R., and Wagenknecht, T. (2004) Location of divergent region 2 on the three-dimensional structure of cardiac muscle ryanodine receptor/calcium release channel. *J. Mol. Biol.* **338,** 533–545
23. Liu, Z., Wang, R., Zhang, J., Chen, S. R., and Wagenknecht, T. (2005) Localization of a disease-associated mutation site in the three-dimensional structure of the cardiac muscle ryanodine receptor. *J. Biol. Chem.* **280,** 37941–37947
24. Serysheva, I. I., Ludtke, S. J., Baker, M. R., Chiu, W., and Hamilton, S. L. (2002) Structure of the voltage-gated L-type Ca^{2+} channel by electron cryomicroscopy. *Proc. Natl. Acad. Sci. U.S.A.* **99,** 10370–10375
25. Paolini, C., Fessenden, J. D., Pessah, I. N., and Franzini-Armstrong, C. (2004) Evidence for conformational coupling between two calcium channels. *Proc. Natl. Acad. Sci. U.S.A.* **101,** 12748–12752
26. Paolini, C., Protasi, F., and Franzini-Armstrong, C. (2004) The relative position of RyR feet and DHPR tetrads in skeletal muscle. *J. Mol. Biol.* **342,** 145–153
27. Zhou, Q., Wang, Q. L., Meng, X., Shu, Y., Jiang, T., Wagenknecht, T., Yin, C. C., Sui, S. F., and Liu, Z. (2008) Structural and functional characterization of ryanodine receptor-natrin toxin interaction. *Biophys. J.* **95,** 4289–4299
28. Meng, X., Wang, G., Viero, C., Wang, Q., Mi, W., Su, X. D., Wagenknecht, T., Williams, A. J., Liu, Z., and Yin, C. C. (2009) CLIC2-RyR1 interaction and structural characterization by cryo-electron microscopy. *J. Mol. Biol.* **387,** 320–334
29. Zhao, M., Li, P., Li, X., Zhang, L., Winkfein, R. J., and Chen, S. R. (1999) Molecular identification of the ryanodine receptor pore-forming segment. *J. Biol. Chem.* **274,** 25971–25974
30. Masumiya, H., Wang, R., Zhang, J., Xiao, B., and Chen, S. R. (2003) Localization of the 12.6-kDa FK506-binding protein (FKBP12.6) binding site to the NH_2-terminal domain of the cardiac Ca^{2+} release channel (ryanodine receptor). *J. Biol. Chem.* **278,** 3786–3792
31. Chen, S. R., Li, X., Ebisawa, K., and Zhang, L. (1997) Functional characterization of the recombinant type 3 Ca^{2+} release channel (ryanodine receptor) expressed in HEK293 cells. *J. Biol. Chem.* **272,** 24234–24246
32. Li, P., and Chen, S. R. (2001) Molecular basis of Ca^{2+} activation of the mouse cardiac Ca^{2+} release channel (ryanodine receptor). *J. Gen. Physiol.* **118,** 33–44
33. Jones, P. P., Jiang, D., Bolstad, J., Hunt, D. J., Zhang, L., Demaurex, N., and Chen, S. R. (2008) Endoplasmic reticulum Ca^{2+} measurements reveal that the cardiac ryanodine receptor mutations linked to cardiac arrhythmia and sudden death alter the threshold for store overload-induced Ca^{2+} release. *Biochem. J.* **412,** 171–178
34. Liu, Z., Wang, R., Tian, X., Zhong, X., Gangopadhyay, J., Cole, R., Ikemoto, N., Chen, S. R., and Wagenknecht, T. (2010) Dynamic, intersubunit interactions between the N-terminal and central mutation regions of cardiac ryanodine receptor. *J. Cell Sci.* **123,** 1775–1784
35. Papadopoulos, S., Leuranguer, V., Bannister, R. A., and Beam, K. G. (2004) Mapping sites of potential proximity between the dihydropyridine receptor and RyR1 in muscle using a cyan fluorescent protein-yellow fluorescent protein tandem as a fluorescence resonance energy transfer probe. *J. Biol. Chem.* **279,** 44046–44056
36. Liu, Z., Zhang, J., Li, P., Chen, S. R., and Wagenknecht, T. (2002) Three-dimensional reconstruction of the recombinant type 2 ryanodine receptor and localization of its divergent region 1. *J. Biol. Chem.* **277,** 46712–46719
37. Zhang, J., Liu, Z., Masumiya, H., Wang, R., Jiang, D., Li, F., Wagenknecht, T., and Chen, S. R. (2003) Three-dimensional localization of divergent region 3 of the ryanodine receptor to the clamp-shaped structures adjacent to the FKBP binding sites. *J. Biol. Chem.* **278,** 14211–14218
38. Wang, R., Chen, W., Cai, S., Zhang, J., Bolstad, J., Wagenknecht, T., Liu, Z., and Chen, S. R. (2007) Localization of an NH_2-terminal disease-causing mutation hot spot to the "clamp" region in the three-dimensional structure of the cardiac ryanodine receptor. *J. Biol. Chem.* **282,** 17785–17793
39. Jones, P. P., Meng, X., Xiao, B., Cai, S., Bolstad, J., Wagenknecht, T., Liu, Z., and Chen, S. R. (2008) Localization of PKA phosphorylation site, Ser-2030-, in the three-dimensional structure of cardiac ryanodine receptor. *Biochem. J.* **410,** 261–270
40. Jiang, D., Xiao, B., Yang, D., Wang, R., Choi, P., Zhang, L., Cheng, H., and Chen, S. R. (2004) RyR2 mutations linked to ventricular tachycardia and sudden death reduce the threshold for store overload-induced Ca^{2+} release (SOICR). *Proc. Natl. Acad. Sci. U.S.A.* **101,** 13062–13067
41. Jiang, D., Wang, R., Xiao, B., Kong, H., Hunt, D. J., Choi, P., Zhang, L., and Chen, S. R. (2005) Enhanced store overload-induced Ca^{2+} release and channel sensitivity to luminal Ca^{2+} activation are common defects of RyR2 mutations linked to ventricular tachycardia and sudden death. *Circ. Res.* **97,** 1173–1181
42. Kong, H., Jones, P. P., Koop, A., Zhang, L., Duff, H. J., and Chen, S. R. (2008) Caffeine induces Ca^{2+} release by reducing the threshold for luminal Ca^{2+} activation of the ryanodine receptor. *Biochem. J.* **414,** 441–452
43. Zorzato, F., Scutari, E., Tegazzin, V., Clementi, E., and Treves, S. (1993) Chlorocresol. An activator of ryanodine receptor-mediated Ca^{2+} release. *Mol. Pharmacol.* **44,** 1192–1201
44. Fessenden, J. D., Perez, C. F., Goth, S., Pessah, I. N., and Allen, P. D. (2003) Identification of a key determinant of ryanodine receptor type 1 required for activation by 4-chloro-m-cresol. *J. Biol. Chem.* **278,** 28727–28735
45. Meissner, G. (1986) Ryanodine activation and inhibition of the Ca^{2+} release channel of sarcoplasmic reticulum. *J. Biol. Chem.* **261,** 6300–6306
46. Rousseau, E., Smith, J. S., and Meissner, G. (1987) Ryanodine modifies conductance and gating behavior of single Ca^{2+} release channel. *Am. J. Physiol.* **253,** C364–C368
47. Radermacher, M., Rao, V., Grassucci, R., Frank, J., Timerman, A. P., Fleischer, S., and Wagenknecht, T. (1994) Cryo-electron microscopy and three-dimensional reconstruction of the calcium release channel/ryanodine receptor from skeletal muscle. *J. Cell Biol.* **127,** 411–423
48. Serysheva, I. I., Orlova, E. V., Chiu, W., Sherman, M. B., Hamilton, S. L., and van Heel, M. (1995) Electron cryomicroscopy and angular reconstitution used to visualize the skeletal muscle calcium release channel. *Nat. Struct. Biol.* **2,** 18–24
49. Samsó, M., Wagenknecht, T., and Allen, P. D. (2005) Internal structure and visualization of transmembrane domains of the RyR1 calcium release channel by cryo-EM. *Nat. Struct. Mol. Biol.* **12,** 539–544
50. Tung, C. C., Lobo, P. A., Kimlicka, L., and Van Petegem, F. (2010) The amino-terminal disease hotspot of ryanodine receptors forms a cytoplasmic vestibule. *Nature* **468,** 585–588
51. Van Petegem, F. (2012) Ryanodine receptors. Structure and function. *J. Biol. Chem.* **287,** 31624–31632
52. Du, G. G., Guo, X., Khanna, V. K., and MacLennan, D. H. (2001) Ryanodine sensitizes the cardiac Ca^{2+} release channel (ryanodine receptor isoform 2) to Ca^{2+} activation and dissociates as the channel is closed by Ca^{2+} depletion. *Proc. Natl. Acad. Sci. U.S.A.* **98,** 13625–13630
53. Masumiya, H., Li, P., Zhang, L., and Chen, S. R. (2001) Ryanodine sensitizes the Ca^{2+} release channel (ryanodine receptor) to Ca^{2+} activation. *J. Biol. Chem.* **276,** 39727–39735